

**Use of Radiation Detection, Measuring, and Imaging Instruments to
Assess Internal Contamination from Intakes of Radionuclides**

**Part IV: Field Tests and Monte Carlo Simulations of
Response of Philips SKYLIGHT Gamma Camera to ⁹⁰Sr**

Prepared by

R. Anigstein, R. H. Olsher, and M. C. Erdman

S. Cohen & Associates
1608 Spring Hill Road
Vienna, Virginia 2218

Under

Purchase Order No. 300819501-01REV

TKC Integration Services, LLC
6628 Brynhurst Drive
Tucker, Georgia 30084

Prepared for

Centers for Disease Control and Prevention
National Center for Environmental Health
Division of Environmental Hazards and Health Effects
Radiation Studies Branch

Under

Contract Number 200-2006-15969.118

Phillip Green
Project Officer

January 6, 2010

Contents

	Page
Preface.	iii
1 Radiation Measurements.	1
1.1 Introduction.	1
1.2 Materials and Equipment.	1
1.2.1 Radioactive Sources.	1
1.2.2 Experimental Apparatus.	2
1.3 Experimental Measurements.	3
2 Monte Carlo Simulations of Experimental Measurements.	5
2.1 Methodology.	5
2.1.1 MCNP Models of Sources.	5
2.1.2 Strontium-90/Yttrium-90 Spectrum.	6
2.2 Comparison of MCNP Simulations with Experimental Measurements.	7
2.3 Alternative Calculations.	7
2.4 Conclusions.	8
References.	10

Tables

1-1. Strontium-90 Sources.	2
2-1. Elemental Composition of Materials in Experimental Apparatus.	6
2-2. Normalized Count Rates from ⁹⁰ Sr Sources on Philips SKYLight Gamma Camera.	7

Figures

1-1. NIST Ampoule(dimensions in cm).	2
2-1. MCNP Model of NIST Ampoule in Water-Filled 50-mL Pyrex Beaker.	5

PREFACE

Part I of the present series described a study to evaluate radiation detection and imaging systems commonly found in hospitals to determine their suitability for rapidly scanning individuals for internal contamination, and to develop recommendations regarding their potential use ([Anigstein et al. 2007a](#)). That report described the measurement of count rates from single discrete radioactive sources of ^{60}Co , ^{137}Cs , ^{192}Ir , and ^{241}Am , using a Philips AXIS gamma camera, an Atomlab thyroid uptake system, and a Ludlum waste monitor. A Monte Carlo computer model of the Philips AXIS camera was developed and validated against the experimental in-air measurements. The model was then applied to calculating count rates on two models of the AXIS camera from radionuclides uniformly distributed in the lungs of a stylized mathematical phantom of the human body, based on the ORNL phantom series described by [Cristy and Eckerman \(1987\)](#).

Part II continued the previous investigation by using realistic anthropomorphic phantoms to study the responses of four instruments to five radionuclides distributed in the lungs ([Anigstein et al. 2007b](#)). The experimental measurements were performed on a Rando Phantom—an anthropomorphic phantom that contains a human skeleton embedded in a tissue-equivalent urethane rubber. The five radionuclides— ^{60}Co , ^{90}Sr , ^{137}Cs , ^{192}Ir , and ^{241}Am —were selected from the 10 nuclides cited by the DOE/NRC Interagency Working Group on Radiological Dispersion Devices as being among the “isotopes of greatest concern” ([DOE/NRC 2003](#), Appendix F). Ten encapsulated sources of each nuclide were placed in pre-drilled holes in the lung region of the phantom. Count rates from each nuclide were measured on the Siemens e.cam Fixed 180 gamma camera, an Atomlab thyroid probe, a Ludlum survey meter, and a Ludlum waste monitor.

As described in part II, the Los Alamos MCNPX computer code ([LANL 2006](#)) was used to calculate calibration factors that relate count rates on these instruments to lung burdens of each of the five nuclides. A mathematical model of each of the instruments was constructed, using engineering drawings and other data obtained from the manufacturers. This model was combined with an MCNP model of a Rando Phantom, constructed from CT scans of this phantom ([Wang et al. 2004](#)). The combined model was used to simulate the response of each instrument to sources in the phantom, and the calculated results were compared to the experimental measurements. The agreement between the calculated and measured responses validated the MCNP models of the four instruments.

Part III ([Anigstein et al. 2007c](#)) extended the earlier investigations to the Philips SKYLIGHT camera. The study was narrowed to three of the five radionuclides reported in Part II: ^{60}Co , ^{137}Cs , and ^{241}Am . That study encompassed measurements and corresponding MCNP simulations of sources of the three nuclides located in the lung region of a Rando Phantom. In addition, measurements and corresponding simulations were carried out with the source capsules in air. The agreement between the calculated and measured responses validated the MCNP model of this instrument.

The current work extends the earlier investigations to the response of the Philips SKYLight camera to bremsstrahlung x rays following the β decay of ^{90}Sr and its short-lived daughter, ^{90}Y . As reported in part II, the count rates recorded by the Siemens e.cam gamma camera exposed to ^{90}Sr sources in the Rando Phantom were approximately 50% higher than the values calculated with the MCNP model. Preliminary studies of count rates recorded by the Philips SKYLight camera exposed to ^{90}Sr sources in air also showed significant discrepancies with the corresponding MCNP calculations. Further measurements and Monte Carlo simulations of ^{90}Sr were therefore undertaken in an attempt to resolve this problem. A calibrated source of ^{90}Sr was procured from the National Institute of Standards and Technology to serve as a primary standard for these studies. Measurements and Monte Carlo simulations of this source, which is in the form of an aqueous solution sealed in a glass ampoule, were supplemented by further studies on the encapsulated sources of ^{90}Sr described in part II.

The authors gratefully acknowledge the support and assistance of a number of individuals and organizations, without whom this work would not have been possible. These include the Nuclear Medicine Division of The Penn State Milton S. Hershey Medical Center, which provided access to their facilities, and Kirsten Felix, nuclear medicine technologist, who assisted in operating the gamma camera. X. George Xu, Associate Professor of Nuclear and Biomedical Engineering, Rensselaer Polytechnic Institute, had earlier provided the MCNP model of a Rando Phantom. Ronald Collé of the Radioactivity Group in the National Institute of Standards and Technology provided information and references on the composition of the SRM ampoules.

Several commercial firms provided valuable support and assistance to the earlier studies which also facilitated the present work. Philips Healthcare provided the design specifications and other data that enabled us to construct a realistic model of the SKYLight camera. Our special thanks go to Jody L. Garrard, Nuclear Medicine Product Manager; Mike Petrillo, Principal Engineer, SPECT Detector Engineering; and John Vesel, all of whom gave generously of their time and effort in support of this project. Joshua Levy, president of The Phantom Laboratory, furnished advice and information, and donated spare parts for the Rando Phantom. Margaret Brown of Kimble Chase LLC provided information on Kimble Glasses.

Chapter 1

RADIATION MEASUREMENTS

1.1 Introduction

Studies presented in part II of the present series of reports ([Anigstein et al. 2007b](#)) reported the count rates measured on the Siemens e.cam gamma camera from encapsulated sources of ^{90}Sr distributed inside the lung region of a Rando Phantom. These count rates were about 50% higher than the results of Monte Carlo simulations using the MCNPX radiation transport code. In contrast, the measured count rates from four α -emitting radionuclides— ^{60}Co , ^{137}Cs , ^{192}Ir , and ^{241}Am —in the same configuration were in good agreement with calculated values.

Additional studies of three of the α -emitting radionuclides— ^{60}Co , ^{137}Cs , and ^{241}Am —performed on the Philips SKYLight gamma camera were presented in part III ([Anigstein et al. 2007c](#)). These studies also showed good agreement between the count rates from these three nuclides in the lung region of a Rando Phantom and the MCNPX simulations. Even better agreement was observed for count rates from unshielded source capsules in an acrylic holder. However, count rates from ^{90}Sr sources in the same holder were about 75% higher than the calculated values. Since further studies on ^{90}Sr were planned, these results were not reported at the time.

The present study was undertaken to resolve these discrepancies. Chapter 1 describes studies to determine the response of the Philips SKYLight camera to $^{90}\text{Sr}/^{90}\text{Y}$ sources in several configurations. The studies were performed at The Penn State Milton S. Hershey Medical Center in Hershey, PA.

1.2 Materials and Equipment

The Rando Phantom and the Philips SKYLight gamma camera were described in part III ([Anigstein et al. 2007c](#)). The radioactive sources and the rest of the experimental apparatus are described below.

1.2.1 Radioactive Sources

Our previous studies utilized custom-made sources, each sealed inside an acrylic rod, 1 cm long \times 4.8 mm in diameter, supplied by Isotope Products Laboratories (IPL) (now Eckert & Ziegler Isotope Products). The sources had been produced by depositing an aqueous solution containing the source material in a cavity drilled along the axis of the cylindrical rod. The water was allowed to evaporate and more solution was added until the desired source strength was reached. Once all the water evaporated, the cavity was sealed with an epoxy resin.¹ A more detailed description of these sources is presented by [Anigstein et al. \(2007b, Section 1.2.2\)](#).

¹ Lissa Tegelman, Isotope Products Laboratories, private communication with Robert Anigstein, SC&A, Inc., 2006.

Because of the low attenuation by the source capsules of photons from the α -emitting nuclides in the previous studies, the exact geometry and elemental composition of the capsules had little impact on the experimental results. In performing the MCNP simulations, it sufficed to represent the activity as a point source located on the center of the axis of each capsule, at the bottom of the cavity. However, bremsstrahlung production is highly dependent on the matrix surrounding the activity.

Seven of the 10 sources originally procured for these studies in 2006 had begun to leak due to radiation damage to the epoxy seals. Such leakage indicates that some of the activity had either been deposited on the wall of the axial cavity or had crept along the wall during the 3 years since the construction of the sources. Since we could not determine the exact distribution of the $^{90}\text{Sr}/^{90}\text{Y}$ activity in the remaining sources, we could not construct an accurate model of these sources. Furthermore, the composition of the acrylic and the resin could be different than the nominal compositions reported for these materials.

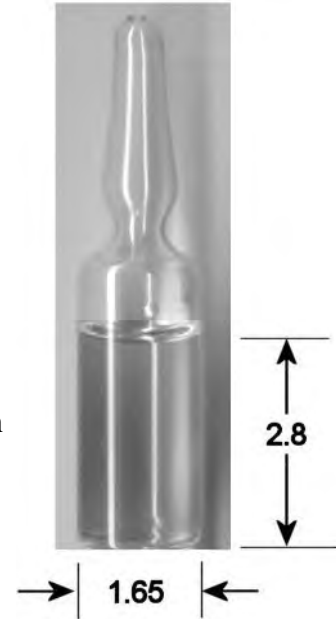


Figure 1-1. NIST Ampoule (dimensions in cm)

We therefore procured a calibrated ^{90}Sr source from the National Institute of Standards and Technology (NIST). This source, described by NIST as “Standard Reference Material® 4239—Strontium-90 Radioactivity Standard,” was furnished as an aqueous solution sealed inside a glass ampoule (see figure 1-1). The activity has an uncertainty of $\pm 0.46\%$

The activities of the various sources used in the experiment are listed in table 1-1.

Table 1-1. Strontium-90 Sources

Date of experiment	Half-life (y)	Supplier	Calibration date	Exposure geometry ^a	Source No.	Calibrated activity (kBq)	Decayed activity (kBq)
		NIST	12/25/06	Beaker	N/A	161.6	161.6
7/11/09	28.79	IPL	2/2/06	Beaker	1	253.7	253.7
					2	253.5	253.4
					1-3	761.0	760.9

^a See text

1.2.2 Experimental Apparatus

The greatest discrepancy between the measured and calculated count rates from $^{90}\text{Sr}/^{90}\text{Y}$ sources observed in our earlier studies occurred when the camera was exposed to the acrylic source capsules in air, the only intervening shields comprising an air gap of approximately 13 cm, the 1.2-mm-thick wall of the acrylic source capsule, the 1.3-mm-thick aluminum window over the NaI(Tl) detector, and the 1.5-mm-thick layer of polytetrafluoroethylene (Teflon) between the

aluminum and the detector. These shields allowed some of the higher-energy electrons emitted by ^{90}Y , which have a cutoff energy of 2,280 keV, to impinge on the crystal.

To ensure that only bremsstrahlung x rays could reach the detector, we suspended the source in a beaker of water, so that the electrons would be totally absorbed within the apparatus. The NIST ampoule was centered in a 50-mL Pyrex beaker filled with deionized water. A separation of 1.1 cm of water was maintained between the ampoule and the beaker, sufficient to absorb the highest-energy β rays, using spacers made from 0.2-mm-thick polyethylene terephthalate (Mylar) sheet. This thin organic material has a negligible interaction with β particles and x rays and could thus be ignored in the MCNP simulations. A similar apparatus, utilizing a 20-mL Pyrex beaker, was used to hold the IPL source capsules. These simple geometries could be readily incorporated into our MCNP model.

1.3 Experimental Measurements

Measurements were performed with the SKYLight camera, using both detectors with the collimators removed. Because the bremsstrahlung x-ray spectrum spanned a wide energy range, two contiguous energy windows were set on the camera. The camera was first peaked using a $^{99\text{m}}\text{Tc}$ source. The upper energy window was centered on the principal β ray, which has an energy of 141.511 keV; the width was set at 67.6%. An ^{241}Am source was used to set the lower energy window. Although the principal β ray of this nuclide has an energy of 59.5412 keV, the spectrum displayed by the camera showed a peak at approximately 62 keV. The low-energy window was centered on this peak; the width was set at 100%.² The energy range spanned by the two windows is estimated to be 28.8–188 keV, based on the β -ray energies of the two nuclides.

In measuring the sources in the beakers, the two heads of the camera were positioned with the aluminum windows 10.4 cm apart. The NIST source in the 50-mL beaker was centered on the detectors. Background counts were taken before and after the measurement, with an identical ampoule filled with plain water positioned in the beaker. In a similar manner, two of the IPL sources in succession were placed inside a water-filled 20-mL beaker. Background counts were recorded before and after the source measurements, with the water-filled beaker remaining in place between the detectors.

In the second group of measurements, three IPL sources were placed in the lung region of the Rando Phantom. The phantom was centered between the two detectors, as described in part III ([Anigstein et al. 2007c](#)). Background counts, with the phantom in position but without sources, were taken before and after the source measurements.

² This procedure was based on instructions for setting windows for nuclides with more than one significant β -ray peak presented in the user's manual for the SKYLight system ([Philips 2007](#)).

Two sets of measurements were taken. First the phantom faced detector 1, with its back to detector 2. Next, the phantom was turned to face detector 2. The reported counts for each view are the averages of the background-corrected counts in each detector.

Chapter 2

MONTE CARLO SIMULATIONS OF EXPERIMENTAL MEASUREMENTS

In this chapter, we discuss the use of Monte Carlo computer models to simulate the experimental measurements presented in chapter 1. The analysis used the mathematical model of the SKYLIGHT camera described in part III (Anigstein et al. 2007c). We computed the radiation response of this model, using the exposure geometries described in chapter 1, and compared the calculated results to the experimental observations.

2.1 Methodology

The methodology was essentially the same as used in the Monte Carlo simulations described in part III (Anigstein et al. 2007c). The only significant differences were the geometry of the sources and the $^{90}\text{Sr}/^{90}\text{Y}$ spectrum.

2.1.1 MCNP Models of Sources

The simplified MCNP model of the NIST ampoule source inside a water-filled 50-mL Pyrex beaker is illustrated in figure 2-1. The dimensions of the beaker, the position of the source capsule, and the diameter of the capsule were determined by measurements on the actual apparatus. The model used the nominal thickness of the ampoule, 0.6 mm, as specified by NIST (2006). The red numbers are the densities of the materials in g/cm^3 .

Since the glass wall of the ampoule was in contact with the $^{90}\text{Sr}/^{90}\text{Y}$ solution, the composition of this glass could affect bremsstrahlung production and could therefore be significant to the analysis. However, NIST (2008b) identified it only as borosilicate glass. NIST (2006) further specified the barium content as less than 2.5%, with “lead oxide”

< 0.02%. Upon further inquiry, we learned that in 1976, NIST purchased a “lifetime” supply of glass ampoules from Kimble Glass, now Kimble Chase LLC (NBS 1976), which is still used to produce the SRM sources.³ According to the purchase order, the glass was specified as Type I.

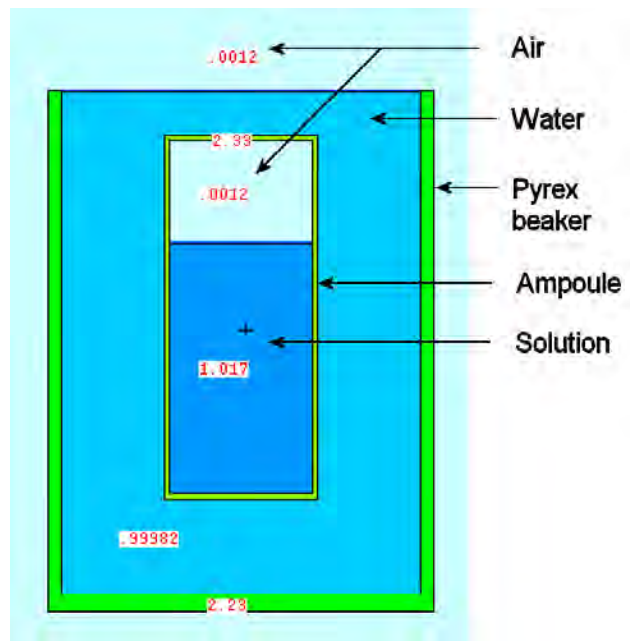


Figure 2-1. MCNP Model of NIST Ampoule in Water-Filled 50-mL Pyrex Beaker

³ Ronald Collé (Research Chemist, Radioactivity Group, (Radioactivity SRM coordination), Ionizing Radiation Division, Physics Laboratory, National Institute of Standards and Technology), private communication with Robert Anigstein, SC&A, Inc., February 24, 2009.

Iroulart (2007), concluded that the glass was Type I, Class B, (there is also a Type I, Class A glass with a different composition). The barium content is variable: NBS (1976) specified it as < 2.5%, while ASTM E 438 – 90 “Standard Specification for Glasses in Laboratory Apparatus,” as cited by Iroulart, specified the concentration of BaO as 0–2%.

To evaluate the potential effect of the uncertainty in the barium content on our study, we performed a sensitivity analysis, using MCNP to simulate the count rates on the Philips SKYLight camera from ampoules with no barium and 2% BaO in the glass. The results showed that an ampoule with 2% BaO produced a count rate that was ~0.5% lower than one with no barium. Since this difference was within the range of the statistical uncertainty of the Monte Carlo analysis, and since there is no reason to believe that barium had been intentionally added to the glass, we did not include it in the final MCNP model. We used the composition of the glass specified in ASTM E 438 – 90 (as cited by Iroulart 2007), without trace constituents, for which only maximum values are specified. The density of Kimble 51A glass, the Type I, Class B glass identified by Iroulart, was provided by Brown (2009).

The elemental compositions and densities of the materials in the MCNP model of the experimental apparatus are listed in table 2-1.

Table 2-1. Elemental Composition of Materials in Experimental Apparatus

Element	NIST ampoule ^a	Pyrex ^b	Solution ^c
H			10.89%
B	3.17%	4.01%	
O	52.11%	53.96%	85.68%
Na	4.54%	2.82%	
Al	3.78%	1.16%	
Si	34.82%	37.72%	
K	0.85%	0.33%	
Ca	0.73%		
Cl			3.43%
Density (g/cm ³)	2.33	2.23	1.02

^a Type I, Class B aluminoborosilicate glass (Iroulart 2007)—see text

^b NIST 2008a

^c Solution containing ⁹⁰Sr/⁹⁰Y consists of 1 M HCL with trace amounts of stable Sr and Y (NIST 2008b)

2.1.2 Strontium-90/Yttrium-90 β Spectrum

The combined ⁹⁰Sr/⁹⁰Y β spectrum was calculated using a modified version of the EDISTR code (Dillman 1980). The original version of the code calculates β spectra using up to 150 logarithmically spaced energy intervals. That procedure emphasizes the low-energy end of the spectrum, which is represented by narrowly spaced energy bins, while the high end of the

spectrum, which is responsible for most of the bremsstrahlung production, is tabulated with much coarser energy increments. We modified the code to tabulate the $^{90}\text{Sr}/^{90}\text{Y}$ spectrum in 456 evenly spaced, 5-keV-wide energy bins, plus a narrow bin just below the 2,280.1 keV cutoff energy for ^{90}Y . This calculated spectrum was used in the Monte Carlo simulations.

2.2 Comparison of MCNP Simulations with Experimental Measurements

The results of the MCNP analyses are listed in table 2-2, together with the observed count rates.

Table 2-2.
Normalized Count Rates from ^{90}Sr Sources on Philips SKYLight Gamma Camera (cps/Bq)

Supplier	Exposure geometry	Source No./ View	MCNP	Experiment	Difference (%) ^a
NIST	Beaker	N/A	7.66e-03	9.55e-03	-20%
IPL	Beaker	1	6.75e-03	8.89e-03	-24%
		2		8.89e-03	-24%
	Rando	Anterior	2.74e-03	3.88e-03	-29%
	Phantom	Posterior	3.13e-03	4.39e-03	-29%

^a MCNP ÷ Experiment - 1

Table 2-2 shows better agreement between the calculated and experimental values than had been obtained in our earlier studies of the response of gamma cameras to ^{90}Sr sources. The best agreement is for the NIST ampoule source in a water-filled beaker, for which the activity of the source, the composition of the materials, and the exposure geometry are known with the greatest precision.

2.3 Alternative Calculations

We investigated the possible use of EGS5 as an alternative to MCNPX for modeling the production of bremsstrahlung x rays by $^{90}\text{Sr}/^{90}\text{Y}$ sources. The EGS (Electron-Gamma Shower) code system is a general purpose package for the Monte Carlo simulation of the coupled transport of electrons and photons in an arbitrary geometry for particles with energies above a few keV up to several hundred GeV (depending on the atomic numbers of the target materials) (Hirayama et al. 2005). EGS was originally developed by the Stanford Linear Accelerator Center at Stanford University, and various versions of the code are widely used in medical physics.

Both EGS5 and MCNPX use a condensed history transport model developed by Berger (1963). In order to follow an electron through a significant energy loss, it is necessary to break the electron's path into many discrete steps which are chosen to be long enough to encompass many collisions but short enough to maintain a small mean energy loss in any one step in order to incorporate multiple-scattering and energy straggling theories. Energy loss and angular deflection of the electron during each slowing down step are sampled from probability

distributions. EGS5 offers several electron transport refinements relative to MCNPX. The transport of delta rays is correlated with the energy of the primary electron in EGS5 but not in MCNPX. In addition, EGS5 employs a dual random hinge approach in which energy loss and multiple elastic scattering are fully decoupled to improve transport over long steps and across boundaries between regions of dissimilar media. The bremsstrahlung cross-sections and angular distributions are similar in both codes.

[Vilches et al. \(2007\)](#) and other authors have observed that it is quite common to find discrepancies among the results of different Monte Carlo programs in specific applications. In order to determine if EGS5 would produce better agreement between measured and calculated values in the present study, we calculated the bremsstrahlung yield from the NIST ampoule source using both EGS5 and MCNPX. We used the two codes to compute the photon current across a cylindrical surface 5 cm in diameter and 5 cm high, centered on the source. The photons were tabulated in 1-keV increments, starting at 30 keV. Over the range 30–188 keV, EGS5 produced a photon current that was 13% lower than that calculated by MCNPX. This indicated that using EGS5 to model the count rate would produce an even greater discrepancy with the experimental results; hence, this code did not offer any advantages over MCNPX in the present application.

2.4 Conclusions

The difference of –20% between the MCNPX simulations of the NIST ampoule source and the experimental measurements is much greater than observed for α -emitting nuclides in simple geometries. The difference gets progressively greater for the IPL sources in a water-filled beaker and in a Rando Phantom.

The better agreement for the NIST source than for the IPL sources in water can be attributed to several factors. Foremost is the fact that the activity in the NIST source is uniformly distributed over the volume of the solution—NIST added stable strontium and yttrium salts to the solution to minimize adsorption of the radioactive ions onto the glass surface. As discussed in section 1.2.1, the exact distribution of the activity in the IPL capsule is uncertain. Since bremsstrahlung production is highly dependent on the composition of the matrix, such uncertainty leads to uncertainty in the photon output. Next, the elemental compositions of the NIST source—both the aqueous solution and the glass ampoule—are known with sufficient accuracy, while the acrylic rod and the epoxy cement used in the IPL capsule may have some unknown components.⁴ Finally, the NIST source has a stated uncertainty of $\pm 0.46\%$ while the IPL sources are certified to $\pm 3.3\%$. The still greater discrepancy between the calculated values for the sources in the Rando Phantom and the measured count rates is attributed to uncertainty in the elemental composition of the material of the phantom and to possible differences between the actual phantom used in the study and the phantom used by [Wang et al. \(2004\)](#) as the basis of their MCNP model.

⁴ The sensitivity analysis of the barium content showed that variability of this element, within the specified limits, did not affect the results.

Despite the observed differences, we believe that the MCNP model can be used to predict the count rates from individuals who have inhaled or ingested ^{90}Sr . The variation among individuals, due both to differences in anatomy and to the variability of the biokinetics of the material after intake, would most likely overshadow any discrepancy in the model. Since the model underestimates the count rates, the application of the model to an exposed individual would tend to somewhat overestimate the intake, and would therefore lead to a conservative assessment. Because it is not known how much of the difference in count rates is attributable to an underestimate by the model, and how much to experimental uncertainty, we do not believe the model prediction should be adjusted upward to produce better agreement with the experimental results.

REFERENCES

Anigstein, R., et al. 2007a. "Use of Radiation Detection, Measuring, and Imaging Instruments to Assess Internal Contamination from Intakes of Radionuclides. Part I: Feasibility Studies." http://www.bt.cdc.gov/radiation/clinicians/evaluation/pdf/Part_I.pdf

Anigstein, R., R. H. Olsher, and J. C. Engdahl. 2007b. "Use of Radiation Detection, Measuring, and Imaging Instruments to Assess Internal Contamination from Intakes of Radionuclides. Part II: Field Tests and Monte Carlo Simulations Using Anthropomorphic Phantoms." http://www.bt.cdc.gov/radiation/clinicians/evaluation/pdf/Part_II.pdf

Anigstein, R., et al. 2007c. "Use of Radiation Detection, Measuring, and Imaging Instruments to Assess Internal Contamination from Intakes of Radionuclides. Part III: Field Tests and Monte Carlo Simulations of Philips SKYLight Gamma Camera." http://www.bt.cdc.gov/radiation/clinicians/evaluation/pdf/Part_III.pdf

Berger, M. J. 1963. "Monte Carlo Calculation of the Penetration and Diffusion of Fast Charged Particles." In B. Alder, S. Fernbach, and M. Rotenberg (Eds.), *Methods in Computational Physics*, Vol. 1. New York: Academic Press.

Brown, M. (Technical Services Manager, Kimble Chase LLC) 2009. <m.brown@kimble-chase.com> "Re: Composition of glass ampules": March 5, 2009, personal e-mail to Robert Anigstein, SC&A, Inc.

Cristy, M., and K. F. Eckerman. 1987. "Specific Absorbed Fractions of Energy at Various Ages from Internal Photon Sources. I. Methods," ORNL/TM-8381/V1. Oak Ridge, TN: Oak Ridge National Laboratory.

Dillman, L. T. 1980. EDISTR—A Computer Program to Obtain a Nuclear Decay Data Base for Radiation Dosimetry, ORNL/TM-6689. RSICC Computer Code Collection [Computer software and manual]. Oak Ridge, TN: Oak Ridge National Laboratory.

The DOE/NRC Interagency Working Group on Radiological Dispersal Devices (DOE/NRC). 2003. "Radiological Dispersal Devices: An Initial Study to Identify Radioactive Materials of Greatest Concern and Approaches to Their Tracking, Tagging, and Disposition." www.ssa.doe.gov/sp70/documents/RDDRPTF14MAY03.pdf

Hirayama, H., et al. 2005. "The EGS5 Code System," SLAC-R-730. Stanford, CA: Stanford Linear Accelerator Center, Stanford University.

Iroulart, M-G. 2007. "Thermodynamic Stability of Radioactivity Standard Solutions," Monographie BIPM-6. Sèvres, France: Bureau International Des Poids et Mesures.

Los Alamos National Laboratory (LANL). 2006. "MCNPX." <http://mcnpx.lanl.gov/>

National Institute of Standards & Technology (NIST). 2008a. "Composition of Pyrex Glass."
<http://physics.nist.gov/cgi-bin/Star/compos.pl?matno=169>

National Institute of Standards & Technology (NIST). 2008b. "Certificate—Standard Reference Material® 4239: Strontium-90 Radioactivity Standard."

Procurement Division, National Bureau of Standards (NBS), U.S. Department of Commerce. 1976. Purchase Order to Kimble Glass, Division of Owens-Illinois (January 29, 1976).

Philips Medical Systems. 2007. "SKYLight® Imaging System User's Manual: A Manual Describing How to Use the SKYLight Imaging System."

Physics Laboratory, Ionizing Radiation Division, National Institute of Standards and Technology (NIST). 2006. "Standard Reference Materials."
<http://physics.nist.gov/Divisions/Div846/srm.html>

Vilches, M., et al. 2007. "Monte Carlo Simulation of the Electron Transport Through Thin Slabs: A Comparative Study of PENELOPE, GEANT3, GEANT4, EGSnrc and MCNPX." *Nuclear Instruments and Methods in Physics Research*, B254(2), 219-230.

Wang, B., X. G. Xu, and C. H. Kim. 2004. "A Monte Carlo CT Model of the Rando Phantom." *American Nuclear Society Transactions*, 90, 473-474.